 CMC, vol.2, no.1, pp.51-63, 2005

Assessment of VOF Strategies for the Analysis of Marangoni Migration, Collisional Coagulation of Droplets and Thermal Wake Effects in Metal Alloys Under Microgravity Conditions

Marcello Lappa[1]

Abstract: A possible approach for the investigation of a number of aspects related to the processing of immiscible alloys, made possible by recent progress in both fields of moving boundary (VOF) methods and speed of computers, is discussed. It can capture in a single numerical treatment and without limiting assumptions both macroscopic information (i.e. the macrophysical problem, heretofore treated in terms of population dynamics) and microscopic details (i.e. the microphysical problem, heretofore treated within the framework of boundary integral methods and/or under the assumption of non-deformable drops). The role played by coalescence in changing the Marangoni migration velocity is discussed together with the possible influence of thermal wake effects for small and large values of the Prandtl number. Some prototype preliminary (very heavy) simulations are used for a better representation of some still unexplored or overlooked aspects.

keyword: Microgravity, Volume of Fluid method, Marangoni effects, Metal alloys.

1 Introduction

Currently the principal area of interest concerning the case of alloys under microgravity conditions deals with a special group of metals (and their organic and transparent surrogates) known as "immiscible alloys" (see, e.g., the authoritative discussions in Ratke, 1993).

When an immiscible alloy is cooled, it demixes into two melts of different compositions and densities (the so-called minority and majority phases). Failure to obtain uniform dispersions of the minority phase through the majority phase in space as well as on the ground is usually referred to as "the phase separation problem"; sometimes this topic is also referred to as "coarsening of the dispersion" (where phase separation stands for *spatial* separation of the phases; the thermodynamic counterpart of the process, i.e. the origin of decomposition in fact is a well-known and essentially understood chemical phenomenon since at least the mid 30^{th} of the last century).

The spatial problem is influenced by a number of possible phenomena related to droplets dynamics and motion: nucleation and ensuing growth, sedimentation and Marangoni migration, shape deformation, agglomeration and coagulation, etc.

Owing to the experimental difficulties in investigating the fluid-dynamics of non-transparent liquids (metal alloys are opaque) a number of mathematical models and methods have appeared over the last years for numerical/theoretical analysis of these aspects when they are disjoint or partially combined.

For instance, the occurrence of coalescence or non-coalescence of colliding droplets was initially investigated within the framework of the lubrication theory (e.g., Davis, Schonberg and Rallison, 1989). The hydrodynamic force resisting the relative motion of two unequal drops was determined for Stokes flow conditions and in the absence of surface Marangoni effect. The drops were assumed to be in near-contact and to have sufficiently high interfacial tension that they remain spherical. The role played by the thermal Marangoni effect in determining the pressure increase in the lubrication film between the drops was considered later by Monti, Savino, Lappa and Tempesta (1998), Monti, Savino, Paterna and Lappa (2000), and Lappa (2004).

The shape of droplets was assumed undeformable in these analyses. In reality, the related interaction can cause drops' deformations even in the case of negligible convective transport and can also substantially alter the migration and sedimentation velocities (owing to deformation and "wake" effects).

[1] MARS (Microgravity Advanced Research and Support Center)
Via Gianturco 31 - 80146, Napoli, Italy
E-mail: marlappa@marscenter.it, marlappa@unina.it

Axi-symmetric thermal wake interaction of two bubbles in a uniform temperature gradient at large Reynolds (Re) and Marangoni (Ma) numbers was studied by Balasubramanian and Subramanian (1999). In this landmark analysis shape deformation was neglected and results were obtained in the limit as Re $\rightarrow \infty$ (potential flow theory).

The literature on the thermocapillary motion of deformable drops is quite limited in contrast to a somewhat related problem concerning the interaction of drops undergoing a buoyancy driven motion. For the latter case numerous recent studies revealed a rich variety of interaction patterns of deformable drops depending on the Bond number and the initial configuration of the system (see, e.g., Manga and Stone, 1993; Rother, Zinchenko and Davis, 1997; Lavrenteva and Nir, 2003). The deformation and motion of two interacting droplets were investigated by these authors in the framework of boundary-integral techniques (with mesh adaptation and stabilization) applicable to the case of slow viscous motion (for the state of the art see, e.g., Zinchenko, Rother and Davis 1997; Bazhlekov, Anderson and Meijer, 2004).

From the foregoing it is evident that current understanding is primarily limited to the motion of single drops and bubbles, or at most two interacting drops and bubbles, which are often assumed to remain spherical (a limit which requires that that interfacial tension forces are large compared to viscous and pressure forces). Moreover, all the studies dealing with the boundary integral method and deformable drops are still limited to the case of very viscous flow (Re $\rightarrow$0).

Initial progress on the simulation of ensembles of droplets has been made by combining theoretical results available for neighboring drops (discussed in the text above) with economical multipole techniques previously used in multiparticle conductivity (Zinchenko, 1994). On such a philosophy are based the so-called "population methods" (see, e.g., the recent contributions by Wu, Ludwig and Ratke, 2003 and Zinchenko and Davis, 2003).

With these methods, drops (a large number) are assumed to be in relative motion due to either gravitational sedimentation or thermal Marangoni migration. They are treated as isolated, microscopic quantities compared to field variables like temperature. Possible collisions are predicted using a "trajectory analysis" to follow the relative motion of pairs of drops. When the drops become sufficiently close, they are assumed to interact with each other due to hydrodynamic disturbances. This hydrodynamic disturbance is modeled in the light of information obtained by means of a separate microscopic approach to the problem (e.g., lubrication theory or boundary integral methods).

Such a philosophy allows a simple and efficient treatment of the problem from a computational point of view and has been applied successfully to situations in which the physical phenomena of interest have a large length scale with respect to the average droplet size. However, the applicability of these methods is limited to the case of very viscous flows.

With regard to all these numerical techniques and the possible approaches discussed in this introduction, it should be pointed out that quasi-steady (very viscous) or non-viscous models are often very idealized conditions, and that a fully transient not simplified analysis would be necessary in order to properly describe and interpret the effective behavior of drops in real experiments and processes. Despite of the aforementioned excellent analyses, an out-standing need is for new scientific approaches not affected by any simplification of the governing equations, applicable to the case of low, high, as well as intermediate values of the Reynolds number, and allowing the treatment of multiple drops and related interplay, deformation and coalescence from a "local" point of view without resorting to dual-scale models.

The present article intends to demonstrate how a moving-boundary (VOF) method is able to predict drops interaction and deformations as well as collision and coagulation events in the presem of temperature gradients, with Marangoni effects and with or without gravity present over a wide range of conditions. These methods and existing computers have only recently been made sufficiently powerful to meet these objectives, including fully three-dimensional simulations of multiple drops. In the last part of the paper some prototype applications are briefly commented with emphasis on aspects still overlooked by the scientific community (like the effect of the Prandtl number) and on the intrinsic potentialities of the proposed numerical approach.

2 VOF - Volume of Fluid Method and moving drops

Historically, pioneering work on VOF (Volume of Fluid or Volume of Fraction, also known as Volume Tracking) methods goes back to Noh and Woodward (1976), but with Hirt and Nichols (1981) and their SOLA-VOF code,

the method became widely used.

As discussed by Rider and Kothe (1998), however, these techniques yet possess solution algorithms that are too often perceived as being heuristic and without mathematical formalism. Part of this misperception lies in the difficulty of applying standard hyperbolic PDE (partial differential equations) numerical analysis tools, which assume algebraic formulations, to methods that are largely geometric in nature (hence, the more appropriate term *volume tracking*). To some extent the lack of formalism in volume tracking methods, manifested as an obscure underlying methodology, has impeded progress in evolutionary algorithmic improvements and application in particular to the case of immiscible metal alloys.

Despite some results being available for the case of rising (1g conditions) and interacting bubbles (Esmaeeli and Tryggvason, 1998, 1999), in fact, the numerical simulation of these aspects in the case of drops sedimenting due to gravity or migrating owing to Marangoni forces can still be regarded as an open task. Despite the widespread use of these methods, VOF-based simulations dealing with these particular aspects are still very rare in literature (rare and excellent efforts have been provided by Gueyffier, Li, Nadim, Scardovelli and Zaleski, 1999; Han and Tryggvason, 1999; Mehdi-Nejad, Mostaghimi and Chandra, 2003 for the case of droplet sedimentation; and Haj-Hariri, Shi and Borhan, 1997 for the case of Marangoni migration).

The present section is devoted to the introduction of a general purpose VOF method able to deal with drop motion due to density difference under normal (or residual) gravity as well as to face with the Marangoni migration phenomena (or both cases). In the light of the above discussion particular care is devoted to formalism.

2.1 The variable material properties approach

The classical VOF formulation (see the authoritative overviews of Rudman, 1997; Rider and Kothe, 1998 and Scardovelli and Zaleski, 1999) relies on the fact that for each additional phase added to the model, a variable is introduced: the volume fraction of the phase in the computational cell. In each control volume (computational cell), the volume fractions of all phases must sum to unity. The fields for all variables and properties are shared by the phases and represent volume-averaged values, as long as the volume fraction of each of the phases is known at each location. Thus the variables and properties in any given cell are either purely representative of one of the phases, or representative of a mixture of the phases depending upon the volume fraction values. Hereafter, for the sake of simplicity the case of interest for the purposes of the present analysis is considered (i.e. only two immiscible phases). If the volume fraction of the phase (1) in the cell is denoted as ϕ, the following three conditions are possible:

$\phi = 0$ (the cell is empty of the fluid (1))

$\phi = 1$ (the cell is full of the fluid (1))

$0 < \phi < 1$ (the cell contains the interface between the fluids)

Based on the local values of ϕ, the appropriate properties and variables are assigned to each control volume within the computational domain. If χ denotes the generic fluid property (e.g., density ρ, dynamic viscosity μ, thermal conductivity λ, specific heat coefficient C_p, etc) the corresponding value in each cell is given by:

$$\chi = \chi_1 \phi + \chi_2 (1 - \phi) \tag{1}$$

this means that the concept of mixed properties is used to interpret the cells containing multiple fluids.

Accordingly, a single momentum equation is solved throughout the domain and the resulting velocity field is shared among the phases, i.e. the governing equations are written for whole computational domain and the different phases are treated as a single fluid with variable material properties:

$$\underline{\nabla} \cdot \underline{V} = 0 \tag{2}$$

$$\frac{\partial (\rho \underline{V})}{\partial t} = -\underline{\nabla} p - \underline{\nabla} \cdot [\rho \underline{V} \underline{V}] + \underline{\nabla} \cdot \left[\mu \left(\underline{\nabla V} + \underline{\nabla V}^T \right) \right] + \underline{F}_g + \underline{F}_\sigma \tag{3}$$

$$\frac{\partial \rho C_P T}{\partial t} = [-\underline{\nabla} \cdot (\rho C_P \underline{V} T) + \underline{\nabla} \cdot (\lambda \underline{\nabla} T)] \tag{4}$$

where the source terms in eq. (3) take into account gravity ($\underline{F}_g$) and surface tension ($\underline{F}_\sigma$) effects respectively.

The phase variable is advected according to a simple transport equation:

$$\frac{D\phi}{Dt} = \frac{\partial \phi}{\partial t} + \underline{V} \cdot \underline{\nabla} \phi = 0 \tag{5}$$

Interfaces are tracked in volume tracking methods by evolving fluid volumes forward in time with solutions of this advection equation.

Since at any time in the solution, exact interface locations are not known (i.e. a given distribution of volume data does not guarantee a unique interface), interface geometry must be inferred, based on local volume data and the assumptions of the particular algorithm, before interfaces can be reconstructed. The reconstructed interface is then used to compute the volume fluxes necessary to integrate the volume evolution equation (5) above, i.e. for better computation of the convective contribution $\underline{V} \cdot \underline{\nabla}\phi$ (these aspects are discussed in section 2.3).

This approach is also known as single region formulation since there is not any need (from a computational point of view) to distinguish the different phases, i.e. to use different computational domains. Along these lines, the reader should be informed of the fact that from a general point of view, two broad strategies exist to deal with interface calculation. One is to use deformable meshes based on a finite volume or finite element representation or body-fitted co-ordinates. The other strategy is to keep the mesh fixed, and to use a separate procedure to describe the position of the interface. From this perspective, the main advantage offered by fixed uniform grids is the great simplicity they afford in the treatment of the bulk fluid regions, away from the interfaces. A further advantage of fixed-grid methods is to avoid the re-meshing that may be necessary whenever interface motion deforms the grid exceedingly.

2.2 The continuum surface force and stress models

The surface tension model used herein is the Continuum Surface Force (CSF) proposed for the first time by Brackbill, Kothe and Zemach (1992). With this model, the addition of surface tension effects to the VOF calculation results in a source term in the momentum equation, i.e. $\underline{F}_\sigma$ in eq. (3).

Surface tension arises as a results of attractive forces between molecules in a fluid. Consider an air bubble in water, for example. Within the bubble, the net force on a molecule due to its neighbors is zero. At the surface, however, the net force is radially inward, and the combined effect of the radial components of force across the entire spherical surface is to make the surface contract, thereby increasing the pressure on the concave side of the surface. The surface tension is a force, acting only at the surface, that is required to maintain equilibrium in such instances. It acts to balance the radially inward intermolecular attractive force with the radially outward pressure gradient force across the surface. In regions where the two fluids are separated, but one of them is not in the form of spherical bubbles, the surface tension acts to decrease the area of the interface. The explanation is basically the same in the case of a liquid-liquid system formed by immiscible fluids.

In practice, the well-known Young-Laplace equation can help the reader to understand the origin of the source term in eq. (3) modeling surface tension forces. Consider for instance the case where the surface tension is constant along the surface and where only the forces normal to the interface are present. The pressure jump across the surface depends on the surface tension coefficient σ and the surface curvature as measured by two radii in orthogonal directions R_1 and R_2:

$$p_2 - p_1 = \sigma \left(\frac{1}{R_1} + \frac{1}{R_2} \right) \tag{6a}$$

i.e.

$$\Delta p = \sigma K \tag{6b}$$

where K is the curvature.

In the light of the foregoing arguments, the surface tension can be written simply in terms of a pressure jump across the surface. This force, in turn, can be expressed as a volume force in eq. (3) using the divergence theorem or a similar artifice to replace the surface force with a volume force. The end of the story is that the interfacial surface forces can be incorporated as body forces per unit volume in the momentum equations rather than as boundary conditions. Instead of a surface tensile force boundary condition applied at a discontinuous interface of the two fluids, a volume force can be used which acts on fluid elements lying within a transition region of finite thickness. This also means that the CSF formulation makes use of the approach that discontinuities can be approximated, without increasing the overall error of approximation, as continuous transitions within which the fluid properties vary smoothly from one fluid to the other over a distance of O(h), where h is a length comparable to the resolution of the computational mesh. Surface tension, therefore, is felt everywhere within the transition region through the volume force included in the momentum equations. A similar mathematical treatment is pos-

sible for the contribution related to surface tension gradients along the interface (Marangoni stress).

It is known in fact that the expression for the stress jump $\underline{f}$, across the interface is given by (see the elegant formalism of Haj-Hariri, Shi and Borhan, 1997):

$$\underline{f} = \left[\sigma K \underline{\hat{n}} - \frac{\partial \sigma}{\partial T}\left(\underline{\underline{I}} - \underline{\hat{n}}\underline{\hat{n}}\right)\cdot \underline{\nabla} T\right] \tag{7}$$

where $\underline{\hat{n}}$ is the unit vector perpendicular to the fluid/fluid interface, K is the curvature and $\underline{\underline{I}}$ is the identity matrix:

$$\underline{\hat{n}} = \frac{\underline{\nabla}\phi}{|\underline{\nabla}\phi|} = (\alpha, \beta) \tag{8}$$

$$K = -\underline{\nabla}\cdot\underline{\hat{n}} = \frac{1}{|\underline{n}|}\left[\frac{\underline{n}}{|\underline{n}|}\cdot\underline{\nabla}|\underline{n}| - \underline{\nabla}\cdot\underline{n}\right] \tag{9}$$

The surface force per unit interfacial area, should be added in the momentum equation as $\underline{f}\,\delta$ where δ is the Dirac-pulse function used to localize the force explicitly at the interface. Using some theoretical artifices (as previously discussed) it can formally be replaced by its volume-distributed counterpart, $\underline{F}$, which satisfies

$$\int_{-\infty}^{\infty} \underline{F}(s)ds = \int_{-\infty}^{\infty} \underline{f}(s)\delta(s)ds \tag{10}$$

where (s) is a level-set function denoting the normal distance from the interface (the interface corresponds to s=0) and δ(s) is the Dirac delta function with its singularity on the interface. Rigorously speaking, f is not defined for non-zero s and must be extended appropriately (e.g., it can be assigned a value of zero for nonzero s because of the presence of the delta function). A comparison of the two integrals in eq. (10) suggests $\underline{F}$=$\underline{f}$·δ(s). Although this expression is of little value in its present form, much can be gained from it if a mollified delta function is used, consistent with the smearing of the interface. Recognizing that

$$\int_{-\infty}^{\infty} \delta(s)ds = \int_{-\infty}^{\infty} \underline{\hat{n}}\cdot\underline{\nabla}\phi ds = 1 \tag{11}$$

the mollified delta function can be defined as $|\underline{\nabla}\phi|$ which, in turn, leads to $\underline{F}$=$\underline{f}|\underline{\nabla}\phi|$.

Thus the second source term in eq. (3) reads:

$$\underline{F_\sigma} = \left[\sigma\, K\, \underline{\hat{n}} - \frac{\partial \sigma}{\partial T}\left(\underline{\underline{I}} - \underline{\hat{n}}\underline{\hat{n}}\right)\cdot\underline{\nabla}T\right]|\underline{\nabla}\phi| \tag{12}$$

where, as previously discussed in the light of the Young-Laplace equation, the first term in the square parenthesis is the normal stress contribution responsible for the shape equilibrium in perpendicular direction, whereas the second is the Marangoni shear stress along the surface that can be responsible for the Marangoni migration phenomena.

It is important to highlight how reliable computation of both K and $\underline{\hat{n}}$ is not easy and special care must be devoted to such computation. Usually the unit normal-vector results from the gradient of a smoothed phase field ϕ (the so-called mollification).

The smoothed VOF function can be computed for instance by convolving ϕ with a B-spline of degree l (Brackbill, Kothe and Zemach, 1992). The smoothed VOF function is given by:

$$\widehat{\phi}_{i,j} = \frac{9}{16}\phi_{ij} + \frac{3}{32}\left(\phi_{ij+1} + \phi_{ij-1} + \phi_{i+1j} + \phi_{i-1j}\right) + \frac{1}{64}\left(\phi_{i+1j+1} + \phi_{i+1j-1} + \phi_{i-1j+1} + \phi_{i-1j-1}\right) \tag{13}$$

This formula may be applied iteratively by multiple passes through the mesh for increased degrees of smoothing.

For further details on these aspect see, e.g., the excellent works of Rider and Kothe (1998) and Gueyffier, Li, Nadim, Scardovelli and Zaleski (1999).

To summarize:

$$\underline{F_\sigma} = \left[\sigma K \underline{\hat{n}} - \frac{\partial \sigma}{\partial T}\left(\underline{\underline{I}} - \underline{\hat{n}}\underline{\hat{n}}\right)\cdot\underline{\nabla}T\right]|\underline{\nabla}\widehat{\phi}| = \sigma K \begin{bmatrix} \frac{\partial\widehat{\phi}}{\partial x} \\ \frac{\partial\widehat{\phi}}{\partial y} \end{bmatrix} - \frac{\partial\sigma}{\partial T}\begin{bmatrix} 1-\alpha\alpha & \alpha\beta \\ \beta\alpha & 1-\beta\beta \end{bmatrix} \cdot \begin{bmatrix} \frac{\partial T}{\partial x} \\ \frac{\partial T}{\partial y} \end{bmatrix} \cdot \sqrt{\left(\frac{\partial\widehat{\phi}}{\partial x}\right)^2 + \left(\frac{\partial\widehat{\phi}}{\partial y}\right)^2} \tag{14}$$

where

$$\alpha = \frac{\partial\widehat{\phi}}{\partial x}\Big/\sqrt{\left(\frac{\partial\widehat{\phi}}{\partial x}\right)^2 + \left(\frac{\partial\widehat{\phi}}{\partial y}\right)^2},$$

$$\beta = \frac{\partial\widehat{\phi}}{\partial y}\Big/\sqrt{\left(\frac{\partial\widehat{\phi}}{\partial x}\right)^2 + \left(\frac{\partial\widehat{\phi}}{\partial y}\right)^2}$$

and $\widehat{\phi}$ is the mollified phase field variable.

The treatment of the source term $\underline{F}_g$ taking into account gravity is relatively simple if compared with the corresponding effort provided for the modeling of $\underline{F}_\sigma$.

In fact the first source terms in eq. (3) simply reads:

$$\underline{F}_g = -\rho \underline{g} = -(\rho_1 \phi + g_2(1-\phi)) \tag{15a}$$

and since, according to the Boussinesq hypothesis (β_T being the thermal expansion coefficient)

$$\rho_i = \rho_{i0}[1-\beta_{Ti}(T-T_o)] \rightarrow$$
$$\underline{F}_g = -\rho \underline{g} = -[\rho_{1o}\phi + \rho_{2o}(1-\phi)] +$$
$$[\rho_{1o}\beta_{T1}\phi + \rho_{2o}\beta_{T2}(1-\phi)](T-T_o) \tag{15b}$$

where the first and the second terms in the square parenthesis can be responsible for sedimentation owing to different density of the phases (e.g., $\rho_{1o} > \rho_{2o}$) and for possible onset of buoyant convection (in non-isothermal conditions), respectively.

Gravity can manifest itself in the process of drop sedimentation in fact in two ways. It has a direct effect on the drop velocity through buoyancy and in a more subtle (but not necessarily insignificant) way through natural convection in the surrounding liquid. This convection can directly affect drop motion and also alter the temperature gradients at the interface.

As anticipated, the main advantage of the above formulation is the topological simplification resulting from the incorporation of the interfacial jump conditions into the bulk equations. This eliminates the rather involved task of generating grids for the interior and exterior domains which must be tracked and reconstructed after each iteration step. With the VOF formulation discussed above, a single grid can be generated without regard for the actual shape of the moving drop. However, as anticipated, a reconstruction technique is required. Different procedures can be used in principle to reconstruct the interface (see the next section).

2.3 Interface reconstruction techniques

The ϕ-field is the only phase information stored in VOF methods. Approximate interface locations are found from a so-called interface reconstruction. This is needed, as anticipated, for advecting ϕ, for determining the local propertied (density, viscosity, etc.) and for better graphical representation. In earlier versions, usually called SLIC (Simple line Interface Method) after Noh and Woodward (1976), interfaces were approximated with either a horizontal or vertical line in each cell. Certainly, such a reconstruction appears rather crude. Nevertheless, it has been used in many versions up to the present day, and many reasonable simulation results were obtained.

The SLIC method approximates interfaces as piecewise constant, where interfaces within each cell are assumed to be lines (or planes in three dimensions) aligned with one of the logical mesh co-ordinates. The Hirt-Nichols (h-n) scheme, as used in the sola-vof code (Hirt and Nichols, 1981), is a variation of the piecewise constant method (piecewise constant/"stair-stepped" approximation). In piecewise constant/stair-stepped methods, interfaces are also forced to align with mesh co-ordinates, but are additionally allowed to "stair-step" (align with more than one mesh co-ordinate) within each cell, depending upon the local distribution of discrete volume data.

A notable feature of the SLIC method is that its volume fluxes can be formulated algebraically, i.e. without needing an exact reconstructed interface position. The volume fluxes can be expressed as a weighted sum of upwind and downwind contributions, depending upon the orientation of the interface relative to the local flow direction. For this case interface reconstruction is used only for visualization purposes.

More accurate reconstructions are possible with PLIC (Piecewise Linear Interface Construction). The interface is approximated by a straight line of arbitrary orientation in each cell. Its orientation is found from the liquid distribution in the neighbor cells; given the volume fraction of one of the two fluids in each computational cell and an estimate of the normal vector to the interface, a planar surface is constructed within the cell having the same normal and dividing the cell into two parts each of which contains the proper volume of one of the two fluids.

This has several advantages: the fluxes of ϕ, with which the phase field ϕ is updated, can be determined more accurately, and essentially free of numerical diffusion. Fluid properties can be allocated accurately. Finally the straight lines also give a graphical representation of good quality.

Fig. 1 shows reconstructed interfaces (shaded regions) for a drop of arbitrary radius (continuous line) using the SLIC and PLIC methods.

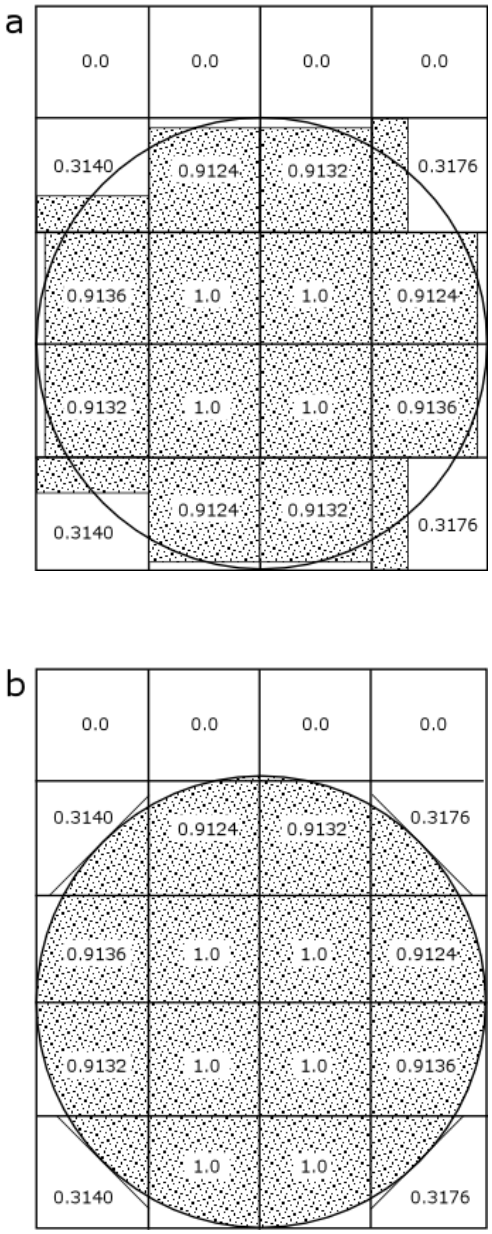

Figure 1 : Reconstructed interfaces (shaded regions) for a drop using the SLIC and PLIC methods. The piecewise constant approximation in SLIC forces the reconstruction to align with selected mesh logical co-ordinates, whereas the piecewise linear approximation in PLIC allows the reconstruction to align naturally with the interface. Numbers in the cells denote volume fractions. (a) SLIC reconstruction. (b) PLIC reconstruction.

2.4 Discretization

The basic numerical algorithm for the solution of eqs. (2-4) is the SMAC splitting method (see, e.g., Lappa, 1997, 2004). For the case under investigation it must be modified to take into account the fact that two phases with different density are present in the computational domain; it consists of the following two steps:

$$\underline{V}^* = \underline{V}^n + \Delta t \frac{1}{\rho^n} \cdot \left[-\underline{\nabla} \cdot [\rho \underline{V}\underline{V}] + \underline{\nabla} \cdot \left[\mu \left(\underline{\nabla V} + \underline{\nabla V}^T \right) \right] + \underline{F}_g + \underline{F}_\sigma^t \right]^n \quad (16)$$

where $\underline{F}_\sigma^t = \left[-\frac{\partial \sigma}{\partial T} \left(\underline{\underline{I}} - \hat{n}\hat{n} \right) \cdot \underline{\nabla} T \right] |\underline{\nabla} \phi|$,

$$\underline{V}^{n+1} = \underline{V}^* + \Delta t \frac{1}{\rho^n} \left[-\underline{\nabla} p + F_\sigma^p \right]^n \quad (17)$$

where $\underline{F}_\sigma^p = [\sigma K \hat{\underline{n}}] |\underline{\nabla} \phi|$
and the elliptic equation reads:

$$\underline{\nabla} \cdot \left[\frac{1}{\rho^n} \underline{\nabla} p \right] = \frac{1}{\Delta t} \underline{\nabla} \cdot \underline{V}^* + \underline{\nabla} \cdot \left[\frac{1}{\rho^n} \underline{F}_\sigma^P \right]^n \quad (18)$$

During each time step, the intermediate velocity field V* is calculated from eq. (16), and used to obtain the pressure through an iterative solution of (18). Subsequently, the new pressure distribution is used in eq. (17) to advance the velocity field to the next time step.

Once the new velocity field, V^{n+1} , is determined, the phase variable is advected according to eq. (5) and the interface reconstruction technique used; this step provides the new distribution ϕ^{n+1}.

Then, the temperature field is updated by using explicit Euler time-marching in eq. (4):

$$T^{n+1} = \frac{\{[\rho C_P T]^n + \Delta t \left[-\underline{\nabla} \cdot (\rho C_P \underline{V} T) + \underline{\nabla} \cdot (\lambda \underline{\nabla} T) \right]^n \}}{[\rho C_P]^{n+1}} \quad (19)$$

3 Relevant examples and insights into the physics of the spatial separation process

As a relevant example, equations (2-5) for the spatially inhomogeneous population of drops in Fig. 2a have been solved to predict spatial phase separation in the presence of a temperature gradient for a dispersion of drops at moderate concentrations, at which both migration and coalescence are important (zero-g conditions). The example demonstrates how the population of drops can be simply reduced to a proper set of initial conditions for the

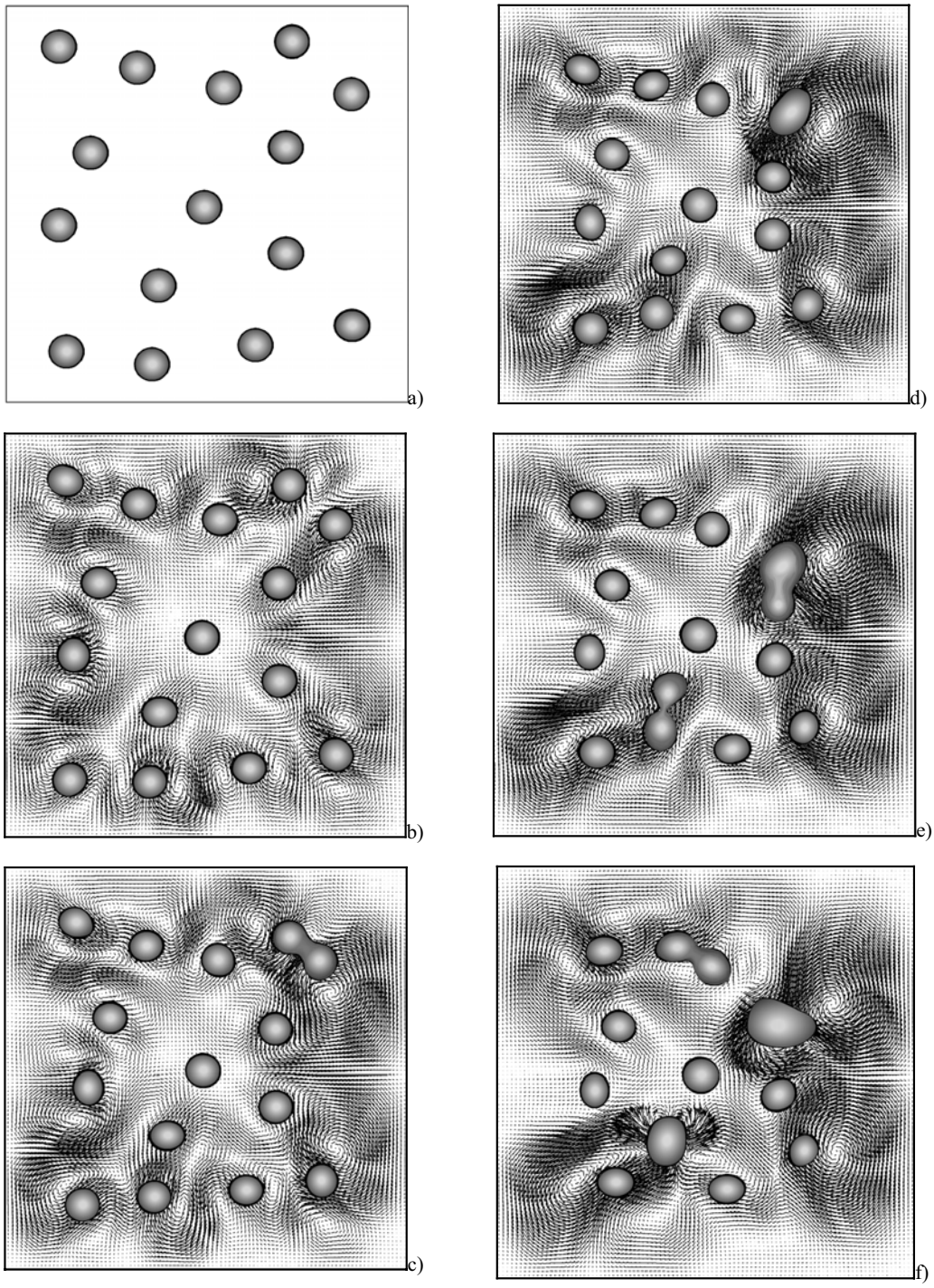

Figure 2 : Bismuth drops in a square container with side L= 1[cm] filled with Zinc melt, initially at T= 750 [K]. The walls of the container are supposed to be cooled with a ramping rate of 1 [K/s] (zero gravity conditions).

phase-variable ϕ (Fig. 2a) and the subsequent dynamics at microscopic scale length can be captured in a natural manner by the simulation (Figs. 2b-f). The case of Zn (1) -Bi (2) system in particular is considered (Table 1).

Table 1 : Physical properties of the Zn (1) -Bi (2) system

T_{m1} [K]	692.7
T_{m2} [K]	544.6
ρ_1 [Kg m^{-3}]	$6.61 \cdot 10^3$
ρ_2 [Kg m^{-3}]	$9.87 \cdot 10^3$
ν_1 [m^2 s^{-1}]	$0.49 \cdot 10^{-6}$
ν_2 [m^2 s^{-1}]	$0.136 \cdot 10^{-6}$
C_{p1} [J $Kg^{-1}K^{-1}$]	$0.495 \cdot 10^3$
C_{p2} [J $Kg^{-1}K^{-1}$]	$0.145 \cdot 10^3$
λ_1 [J $m^{-1}s^{-1}K^{-1}$]	15.8
λ_2 [J $m^{-1}s^{-1}K^{-1}$]	58.1
σ [dyne m^{-1}]	$\cong 6 \cdot 10^4$
σ_T[dyne $m^{-1}K^{-1}$]	$\cong 10$

The container is a square cell with side L= 1[cm] filled with the melt, initially at T= 750 [K]. The walls of the container are supposed to be cooled with a ramping rate of 1 [K/s]. The PLIC scheme is used for interface reconstruction.

Figs. 2 show that all the Bismuth drops migrate towards the center of the container due to "Marangoni migration" (among other things, these results could provide a possible theoretical justification for the experimental behavior shown in Fig. 3).

It is known that on the ground, droplets coalescence strengthens the mechanisms leading to phase separation since heavier drops are formed with increased velocity of sedimentation. As described by Stokes' law, in fact, the sedimentation velocity of the heavy droplets increases as the square of the particle diameter, so big droplets settle much more rapidly than small ones. When droplets of different diameters and thus different sedimentation velocity collide, they coagulate to form bigger droplets which settle even more rapidly.

The present simulations show that also in the absence of gravity the effect is similar; drops coalescence in space leads to larger drops and this increases the velocity of Marangoni migration owing to the increase of the interface where the surface tension stresses act propelling the drop (the reader may consider eqs. (20) and (21) as representative of the effect of the radius on the Marangoni

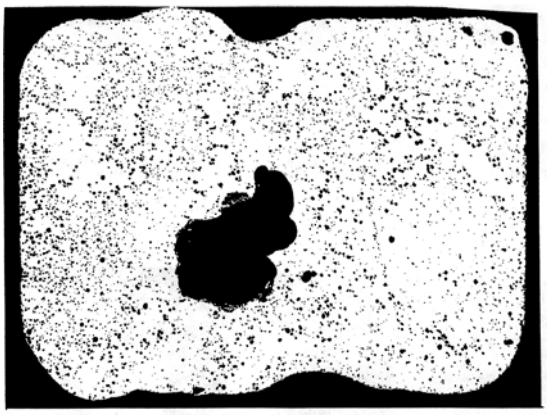

Figure 3 : Examples of separation occurred during radial solidification processes in microgravity (from H.U. Walter; ESA SP-219 1984, p. 47).

migration for the cases Ma$\rightarrow$0 and Ma$\rightarrow \infty$: the migration velocity is proportional to R or to R^3 for small or large values of Ma respectively).

It is known (Young, Goldstein and Block 1959), in fact, that in the limit of zero Marangoni number (i.e. with negligible convective transport effects) the droplet velocity U within an unbounded fluid medium in the laboratory co-ordinate frame is related to the uniform temperature gradient $\partial T/\partial x$ by

$$U_S = -\left[\frac{2R\left.\frac{\partial\sigma}{\partial T}\right|_{drop}}{\mu_2\left(\frac{\lambda_1}{\lambda_2}+2\right)\left(3\frac{\mu_1}{\mu_2}+2\right)}\right]\frac{\partial T}{\partial x} \tag{20}$$

In this expression, $\partial\sigma/\partial T_{drop}$ represents the variation of interfacial tension with temperature at some reference temperature (e.g., that at the center of the drop), μ_2 and λ_2 are the viscosity and the thermal conductivity of the external fluid, respectively. Equation (20) is valid as long as the drop remains sufficiently small that convective transport of heat and momentum can be neglected compared to molecular transport of these quantities, i.e. for small values of the Reynolds number, $2\rho_2 U_S R/\mu_2$, and the Marangoni number, Ma=Re·Pr= $2U_S R/\alpha_2$, where ρ_2 and α_2 denote the density and thermal diffusivity of the external fluid, respectively, and Pr= ν_2/α_2.

In the limit as Ma$\rightarrow \infty$ the velocity of a drop is proportional to the square of the temperature gradient and the cube of the radius of the drop (Balasubramanian and Sub-

ramanian (2000)):

$$U_S = \frac{4\left|\sigma_T\right|^2 R^3 h(\delta)}{\mu_2^2 \frac{\alpha_1}{\alpha_2}\left(2+3\frac{\mu_1}{\mu_2}\right)^2 (1+\delta)^2}\left(\frac{\partial T}{\partial x}\right)^2 \tag{21}$$

where $\delta = \sqrt{\frac{\alpha_1}{\alpha_2}}\frac{\lambda_2}{\lambda_1}$

and (h(δ)= 5.68 10^{-3} for δ=0; 6.42 10^{-3} for δ=0.5; 7.75 10^{-3} for δ=5; 8.26 10^{-3} for $\delta \to \infty$).

Between these two limiting situations, analytical relationships are not available and information about the phenomena can be only provided by numerical methods such as the VOF technique discussed in section 2.

The application of the present VOF method, however goes beyond the possibility to estimate the migration velocity for effective values of the Reynolds number or the possibility to investigate how coalescence strengthens the phase separation process. It can also provide interesting information concerning the role played by the thermal wakes produced beyond the drops.

As mentioned in the introduction, this problem has been considered for the first time in the landmark study of Balasubramanian and Subramanian (1999). Their analysis considered two bubbles moving in the direction of the temperature gradient and assumed to interact axisymmetrically via the influence of the thermal wake of the leading bubble on the trailing bubble. This analysis is very important since it was proven that the thermal wake of the leading bubble can induces a non-monotonic temperature field on the surface of the trailing bubble. The effective temperature gradient on the trailing bubble is weakened and hence its migration speed is reduced compared to the case when it is isolated.

Similar behaviors are also expected in the case of interacting drops. The temperature gradient in the wake will be weaker than the applied gradient. The thermal wake field of the leading drop will wrap around the trailing drop having a significant impact on its motion.

In the aforementioned landmark analysis shape deformation was neglected and results were obtained in the limit as Ma$\to \infty$ within the framework of a potential flow theory.

Numerical simulations carried out herein for cases of technological interest, show that, in practice, different situations may arise according to the Prandtl number (Pr=ν/α where ν and α are the kinematic viscosity and the thermal diffusivity of the majority phase respectively).

Table 2 : Physical properties of the Ethyl-alcohol (1) - Silicone-oil 1 [cs] (2) system

ρ_1 [Kg m^{-3}]	$0.86 \cdot 10^3$
ρ_2 [Kg m^{-3}]	$0.816 \cdot 10^3$
ν_1 [m^2 s^{-1}]	$1.16 \cdot 10^{-6}$
ν_2 [m^2 s^{-1}]	$1.0 \cdot 10^{-6}$
C_{p1} [J $Kg^{-1}K^{-1}$]	$2.11 \cdot 10^3$
C_{p2} [J $Kg^{-1}K^{-1}$]	$2.05 \cdot 10^3$
λ_1 [J $m^{-1}s^{-1}K^{-1}$]	$1.8 \cdot 10^{-1}$
λ_2 [J $m^{-1}s^{-1}K^{-1}$]	$1.0 \cdot 10^{-1}$
σ [dyne m^{-1}]	$\cong 5 \cdot 10^2$
σ_T[dyne $m^{-1}K^{-1}$]	≅1.5

If Pr is low (Pr<<1 in the case of liquid metals and semiconductors), thermal wake effects are generally negligible and the only mechanisms playing an effective role in affecting the phase separation phenomena are Marangoni motion of the drops and the coagulation events. This aspect is confirmed by the simulation for the case Zn-Bi illustrated before.

For such case in fact, the temperature field is almost diffusive. This is due to the fact that, owing to the large thermal diffusivity of the materials, temperature distortions induced by the motion of the drops are rapidly destroyed (they are spread over large regions).

If large Prandtl number fluids are considered (transparent and/or organic liquids), on the contrary one can expect that thermal wake effects become important. Owing to the small thermal diffusivity of these liquids, the distortion induced in the temperature field in fact should be somehow "frozen" with respect to the times with which the drops migrate within the container.

To check this aspect some simulations have been carried out in the case of an immiscible alloy of Silicone oil and Ethyl-alcohol (Pr>>1, see Table 2).

Figs. 4 show the case of a single drop that migrates in the absence of gravity (0g) towards the hot region owing to thermocapillary effects.

Initially, the temperature profile is linearly stratified ($\partial T/\partial x$=0.1 [K cm^{-1}]), the drop (R=0.5 [cm]) is of Ethyl-alcohol and the surrounding matrix is Silicone oil 1 [cs].

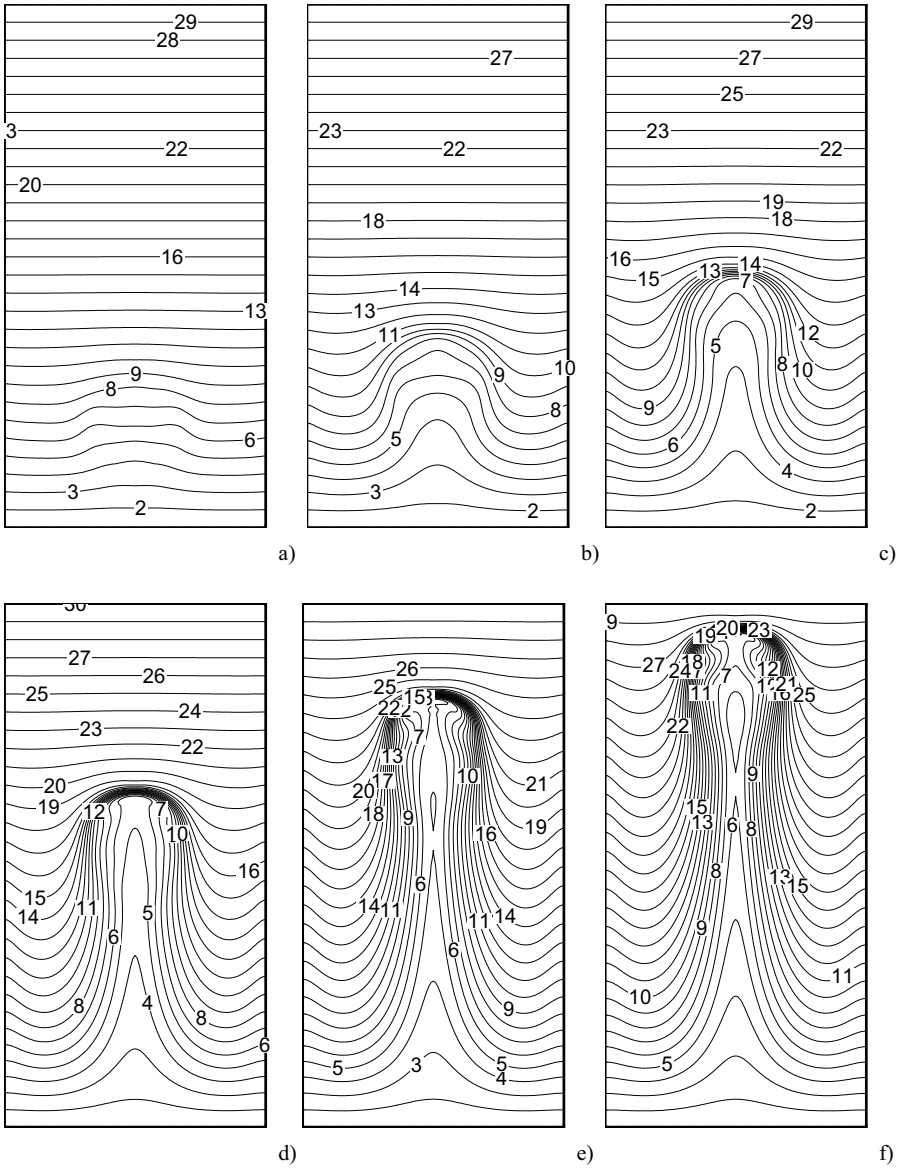

Figure 4 : Drop of Ethyl alcohol (R= 0.5 [cm]) migrating in Silicone oil 1 [cs] under the effect of temperature gradient $\partial T/\partial x$=0.1 [K cm^{-1}], microgravity conditions - Temperature field: (a) 4.2 [s], (b) 10.1 [s], (c) 16 [s], (d) 21.9 [s], (e) 27.8, (f) 33.7 [s] (level 1→T=0 [˚ C], level 30→T=0.6 [˚ C]).

The figures show that the temperature profile near the front pole of the drop is highly distorted with respect to the stratified temperature profile so that the drop does not migrate as in an unbounded medium of infinite extent subjected to a uniform temperature gradient.

Since the energy exchange by heat between the drop and surrounding phase is very small (both the liquids have small values of the thermal conductivity), the drop tends to stay cold. Accordingly, the external isotherms encountered by the drop during the migration process do not penetrate within the drop and fold over it. The drop pushes the isotherms and constrains them in a narrow thermal boundary layer surrounding the drop and having a steep normal temperature gradient.

Figs. 4 also show how the external fluid creates a cold wake that extends behind the drop and entrains the hot region. This wake can be responsible for the aforementioned effects of thermal gradient weakening on a trailing

drop.

4 Conclusions

In the present paper a numerical method able to handle the spatial separation problem in immiscible alloys as well as to elucidate the related mechanisms over a large range of conditions has been carefully introduced. The VOF strategy offers significant advantages with respect to the other methods currently used in the investigation of these topics, even if it still requires parallel (multiprocessor) computations and very long (often prohibitive) simulation times.

The analysis has progressed with the aid and support of a prototype application concerning the case of Zn-Bi, used for a better representation of some mechanisms.

For non-homogeneous and concentrated dispersions of deformable drops, Marangoni migration causes spatial as well as temporal variation in the distribution of drops at macroscopic scale. Superimposed on this are shape distortion, thermal wake effects and coalescence phenomena at microscopic scale. The present analysis demonstrates how the application of the VOF methods to these problems can capture both the macro and micro-physical problem in a single numerical treatment.

Additional studies are required to extend these methods to the case of electric and magnetic fields (sometimes used by researchers to weaken the spatial separation mechanisms), to model the possible presence of dissolution phenomena driven by lack of compositional equilibrium when a droplet moves to regions with a different temperature (some initial effort along these lines has been provided by Lappa and Piccolo, 2004 for the case of a single drop), and finally to model the effect of high frequency vibrations (a still unexplored effect that can suppress coalescence phenomena and can be used as an additional means for control of coarsening kinetics).

Acknowledgement: The author would like to thank Dr. G. De Chiara (Mars Center) for the technical support provided in preparing the figures.

References

Balasubramaniam, R.; Subramanian, R. S. (2000): The migration of a drop in a uniform temperature gradient at large Marangoni numbers, *Phys. Fluids*, Vol. 12(4), pp. 733-743.

Balasubramaniam, R.; Subramanian, R. S. (1999): Axisymmetric thermal wake interaction of two bubbles in a uniform temperature gradient at large Reynolds and Marangoni numbers, *Phys. Fluids*, Vol. 11(10), pp. 2856-2864.

Bazhlekov, I. B.; Anderson, P. D.; Meijer, H. E. H. (2004): Nonsingular boundary integral method for deformable drops in viscous flows, *Phys. Fluids*, Vol. 16(4), pp. 1064-1081.

Brackbill, J. U.; Kothe, D. B.; Zemach, C. (1992): A Continuum Method for Modeling Surface Tension, *J. Comput. Phys*., Vol. 100 (2), pp. 335-354.

Davis, R. H.; Schonberg, J. A.; Rallison, J. M. (1989): The lubrication force between two viscous drops, *Phys. Fluids*, Vol. 1(1), pp. 77-81.

Esmaeeli, A.; Tryggvason, G. (1998): Direct Numerical Simulations of Bubbly Flows. Part I—Low Reynolds Number Arrays, *J. Fluid Mech.*, Vol. 377, pp. 313-345.

Esmaeeli, A.; Tryggvason, G. (1999): Direct Numerical Simulations of Bubbly Flows. Part II—Moderate Reynolds Number Arrays, *J. Fluid Mech*., Vol. 385, pp. 325-358.

Gueyffier, D.; Li, J.; Nadim, A.; Scardovelli, S.; Zaleski, S. (1999): Volume of Fluid interface tracking with smoothed surface stress methods for three-dimensional flows, *J. Comput. Phys.*, Vol. 152, pp. 423-456

Haj-Hariri, H.; Shi, Q.; Borhan, A. (1997): Thermocapillary motion of deformable drops at finite Reynolds and Marangoni numbers, *Phys. Fluids*, Vol. 9 (4), pp. 845-855.

Han, J.; Tryggvason, G. (1999): Secondary breakup of axisymmetric liquid drops. I. Acceleration by a constant body force, *Phys. Fluids*, Vol. 11(12), pp. 3650-3667.

Hirt, C. W.; Nicholsl, B. D. (1981): Volume of Fluid (VOF) Method for the Dynamics of Free Boundaries, *J. Comput. Phys.*, Vol. 39, pp. 201-225.

Lappa, M. (1997): Strategies for parallelizing the three-dimensional Navier-Stokes equations on the Cray T3E, *Science and Supercomputing at CINECA*, Vol. 11, pp. 326-340.

Lappa, M. (2004): Fluids, Materials & Microgravity: Numerical techniques and insights into the physics, Elsevier Science (2004, Oxford), pp: 1-520.

Lappa, M.; Piccolo, C. (2004): Higher modes of Mixed Buoyant-Marangoni unstable convection originated from

a droplet dissolving in a liquid/liquid system with miscibility gap, *Phys. Fluids*, Vol. 16(12), pp. 4262-4272.

Lavrenteva, O. M.; Nir, A. (2003): Axisymmetric thermal wake interaction of two drops in a gravity field at low Reynolds and high Peclet numbers, *Phys. Fluids* Vol. 15 (10), pp. 3006-3014.

Manga, M. H.; Stone, H. A. (1993): Buoyancy-driven interactions between two deformable viscous drops, *J. Fluid Mech*., Vol. 256, pp. 647-683.

Monti, R.; Savino, R.; Lappa, M.; Tempesta, S. (1998): Behaviour of drops in contact with liquid surfaces at non wetting conditions; *Phys. Fluids*, Vol. 10 (11), pp. 2786-2796.

Monti, R.; Savino, R.; Paterna, D.; Lappa, M. (2000): New features of drops dynamics under Marangoni effect, Recent Research Developments in Fluid Dynamics, Transworld Research Network, Trivandrum, India, Vol.3, pp. 15-32.

Mehdi-Nejad, V.; Mostaghimi, J.; Chandra, S. (2003): Two-fluid Heat Transfer Based on a Volume Tracking advection Algorithm, 9th International Conference on Liquid Atomization and Spray Systems.

Noh, W. F.; Woodward, P. R. (1976): SLIC (simple line interface method), in *Lecture Notes in Phys., Vol. 5*9, edited by A. I. van de Vooren and P. J. Zandbergen (Springer-Verlag, Berlin/New York, 1976), p. 330.

Ratke, L., editor (1993): Decomposition, Phase separation, Solidification of immiscible liquid alloys, in Immiscible liquid metals and organics, Proceedings of an international workshop organized by the ESA expert working group, "Immiscible alloys" held in the Physikzentrum, Bad Honnef 1992, Germany, 1993: 3-34.

Rider, W. J.; Kothe, D. B. (1998): Reconstructing Volume Tracking, *J. Comput. Phys.*, Vol. 141, pp. 112-152.

Rother M. A.; Zinchenko, A. Z.; Davis, R. H. (1997): Buoyancy-driven coalescence of slightly deformable drops, *J. Fluid Mech.*, Vol. 346, pp. 117-148.

Rudman, M. (1997): Volume-tracking methods for interfacial flow calculations, *Int. J. Numer. Meth. Fluids*, Vol.24, pp. 671-691.

Scardovelli, S.; Zaleski, S. (1999): Direct numerical simulation of free surface and interfacial flow, *Ann. Rev. Fluid. Mech.*, Vol. 31, pp. 567-603.

Subramanian, R. S.; Balasubramaniam, R. (2001): The Motion of Bubbles and Drops in Reduced Gravity, Cambridge University Press, Cambridge, UK.

Subramanian, R. S.; Zhang, L.; Balasubramaniam, R. (2001): Mass Transport from a Drop Executing Thermocapillary Motion, *Microgravity Sci. and Tech.*, Vol. XII (3/4), pp. 107-115.

Wu, M.; Ludwig, A.; Ratke, L. (2003): Modelling the solidification of hypermonotectic alloys, *Modelling Simul. Mater. Sci. Eng.*, Vol. 11(5), pp. 755-769.

Young, N. O.; Goldstein, J. S.; Block, M. J. (1959): The motion of bubbles in a vertical temperature gradient, *J. Fluid Mech*, Vol. 6, pp. 350-360.

Zinchenko A. Z. (1994): An efficient algorithm for calculating multiparticle thermal interaction in a concentrated dispersion of spheres, *J. Comput. Phys*. Vol. 111, pp. 120-134.

Zinchenko, A. Z.; Davis, R. H. (2003): Large-scale Simulations of Concentrated Emulsion Flows, *Phil. Trans. R. Soc. Lond.*, Vol. 361, pp. 813-845.

Zinchenko, A. Z.; Rother, M. A.; Davis, R. H. (1997): A novel boundary-integral algorithm for viscous interactions of deformable drops, *Phys. Fluids*, Vol. 9, pp. 1493-1515.